# Tomographic Reconstruction of Plasma Equilibria and MHD-Modes at WENDELSTEIN 7-AS

**C. Görner**, M. Anton, J. Geiger, W. von der Linden, A. Weller, S. Zoletnik❖, W7AS-Team

*Max-Planck-Institut für Plasmaphysik, EURATOM Association, D-85748 Garching*

*❖ KFKI-Research Inst., Dept. of Plasma Physics, P.O. Box 49, Budapest-114, HUNGARY*

## I. Introduction

The usage of soft-X radiation for detection of MHD-activities in a plasma and for mapping of plasma equilibrium flux surfaces is a widely applied method on fusion devices. The specific magnetic configuration of W7-AS is the result of the optimization procedure for the stellarator design and, compared with the axial-symmetric tokamak configuration, the flux surfaces are three-dimensional and are characteristically shaped in a poloidal plane, such that a tomographic system needs an enhanced poloidal resolution. To achieve proper plasma imaging for the soft-X radiation, a small sized camera system was installed inside the vacuum vessel to overcome the technical restriction of access from the inboard side of the torus. The system consists of 10 cameras with a total sum of 320 channels and therefore a good spatial resolution in both the radial and poloidal direction is obtained. Together with a well balanced distribution over the poloidal plane, tomographic reconstruction of the soft-X emissivity distribution (6μm Be filter) can be done without additional assumptions about the topology.

In this paper we introduce the camera system and the numerical algorithm, applied for the tomographic reconstruction. Additional data processing is also presented. With the whole tomographic system, comprising the hard- and software, we show some applications to

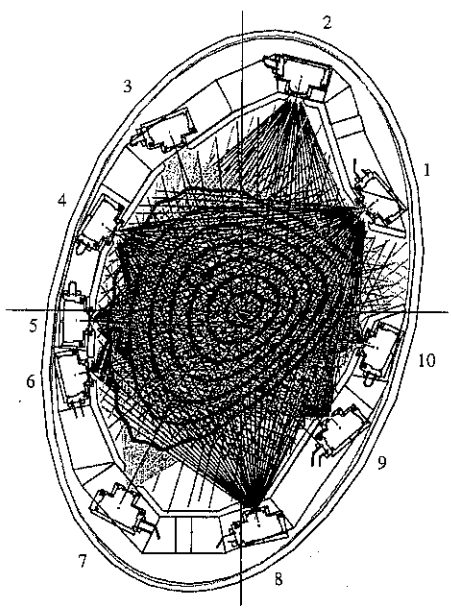


*Fig. 1: 10 camera tomographic system at W7-AS. All 320 lines of sight are drawn. Typical $\iota \approx 1/3$ flux surfaces are additional plotted. The surrounding ellipse is the W7-AS vessel.*

measurements of the equilibrium flux contours and MHD-activities, seen in the stellarator W7-AS.

## II. The 10-camera tomographic system at W7-AS

Figure 1 shows an overview of the hardware of the tomographic system together with the idealized lines of sight of the X-ray detectors. The spatial resolution is comparable with the separation between two neighbouring lines. Data acquisition is performed with a sampling rate of up to 200kHz in time windows with a typical duration of about 50ms (defined by a maximum total data amount of 8MByte per shot).

Three different algorithms for the 10-camera tomography and additional techniques to extract the relevant physical data are used, because different reconstruction problems may require an appropriate algorithm. A choice can be made between algorithms using first order regularisation [1], which tries to avoid steep gradients, a minimum Fisher-information regularisation scheme [2] and the maximum entropy [3, 4] solution.

$$\Lambda_{\mathrm{LinReg}} = \frac{1}{2}\chi^2 + \alpha_R R \qquad R = \int \|\nabla \rho\|^2 \qquad \text{1. order regularisation}$$

$$\Lambda_{\mathrm{MinFisher}} = \frac{1}{2}\chi^2 + \alpha_R I_F \qquad I_F = \int \frac{g'(x)^2}{g(x)} dx \qquad \text{min. Fisher-information}$$

$$\Lambda_{\mathrm{MaxEnt}} = \frac{1}{2}\chi^2 - \alpha_R S \qquad S = \sum_{i=1}^{N_p} \left[ \rho_i - m_i - \rho_i \ln \frac{\rho_i}{m_i} \right] \qquad \text{max. entropy}$$

Maximum Entropy is not a widely used algorithm, because of the long numerical calculations. On the other side, it is the only algorithm, implemented such, that the result is a real mathematical result without the need of guessing the regularisation parameter. Additionally, error bars for the reconstructed distribution are obtained by this method.

For visualisation and quantitative analysis, additional processing is necessary. This includes the implementation of different meshes and expansion functions of the emissivity to be reconstructed, singular value decomposition (SVD), filtering in the frequency-space and error calculations for the case of maximum entropy reconstructions. SVD thereby is the most important method, to extract the fluctuating part of the emissivity attributed to MHD-modes from a sequence of reconstructions. In order to check the reliability, simulated plasma radiation distributions were used.

## III. Equilibrium reconstructions

Concerning equilibrium effects, quantitative measurements of the magnetic surface struc-

ture were made. Two effects have been investigated in particular: the change of the plasma shape due to toroidal currents and the effect of the Shafranov-shift, depending on the plasma beta. The minimization of the Shafranov-shift is one of the most important optimization criteria of W7-AS. The comparison between reconstructions and equilibrium calculations [5] was made for a mean plasma radius were SX-profiles have steep gradients. For both cases very good agreement was observed. Only minor differences in the reconstructions was observed in comparing the three tomographic algorithms mentioned above.

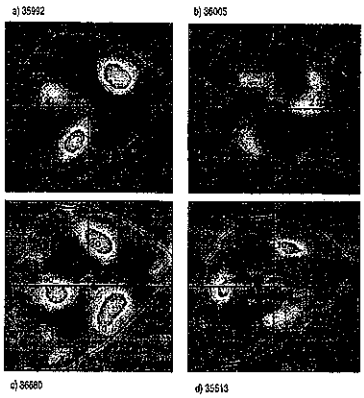


***Figure 2: Four different modes with poloidal mode number m = 3.*** *a) and b) GAE, c) pressure driven mode and d) tearing mode. The plotted flux surface is at normalized radius of 0.75.*

## IV. MHD-activities

The physics issues addressed in this paper comprise, firstly, different kinds of MHD-instabilities including pressure- and current-driven modes and fast particle driven global Alfvén eigenmodes (GAE). An example is shown figure 2, where different modes are plotted for the case of m = 3. GAE-modes usually extend over a large part of the plasma cross section, whereas tearing modes and pressure driven modes are localized around a rational surface.

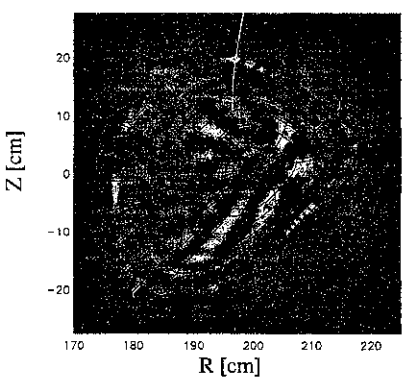


***Figure 3: GAE with m=9.*** *Fourier-expansion in the magnetic angle is used. There for only the radius-dependent phase is a measured quantity. The phase agrees with lines of constant magnetic angle.*

In the case of GAE modes, the reconstruction of the radial and poloidal mode structures, i.e. the determination of the poloidal mode number (m) and the radial eigenfunction, a variety of peaks found in the Alfvén spectrum were analysed. Most of the peaks correspond to the lowest (m,n)-modes expected from theory, but also higher m-numbers and modes with different radial structure were observed. At Wendelstein 7-AS, GAE-modes are commonly seen with neutral beam heating, and the main features are compatible with theoretical predictions, see [6]. With the new tomographic system,

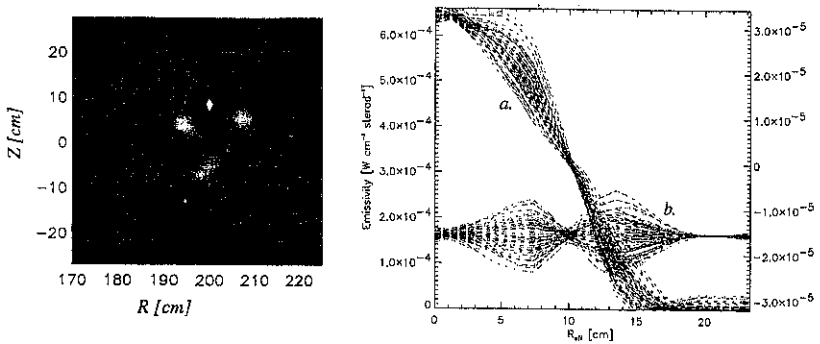


***Figure 4: Radial mode structure found in shot #35982.*** *Left: SVD-filtered picture of the fluctuating emissivity. The solid line corresponds to magnetic angle of* $\theta = 40^{\circ}$.
*Right: Profiles of the total emissivity profile (a., left axis) and the fluctuations (b., right axis) at different time points (at* $\theta = 40^{\circ}$*). For the total profile, the fluctuations are magnified by a factor of 10.*

more complex mode structures can be assessed. For example, figure 3 shows an (m=9)-GAE mode that shows up together with a (m=3) and (m=6) mode (not plotted). Another example, Figure 4, shows two (m=3)-GAEs: one with a radial node at about $R_{eff}$=10cm and the second without node are observed simultaneously. In both discharges, m = (3,6,9) and m = (3,3 with radial node), the modes propagate at different frequencies, that seem to develop independently during the live time of the modes.

## References

[1] S. Zoletnik and S. Kálvin. *Rev. Sci. Instrum.*, **64**(5):1208–1212, 1993.

[2] M. Anton, H. Weisen, M. J. Dutch, W. von der Linden, F. Buhlmann, R. Chavan, B. Marletz, P. Marmillod, and P. Paris. *Plasma Physics of Controlled Fusion*, **38**:1849 – 1878, 1996.

[3] W. von der Linden. *Applied Physics A*, **60**:155 – 165, 1994.

[4] K. Ertl, W. von der Linden, V. Dose, and A. Weller. *Nuclear Fusion*, **36**(11):1477 – 1488, 1996.

[5] H. Callaghan, J. Geiger, C. Görner, J. V. Hofmann, R. Jaenicke, and A. Weller. *this conference.*

[6] A. Weller, D. A. Spong, R. Jaenicke, A. Lazeros, F. P. Penningsfeld, S. Sattler, W7-AS Team, and NBI-Group. *Physical Review Letters*, **72**(8):1220, 1994.